Development/Plasticity/Repair

Negative Guidance Factor-Induced Macropinocytosis in the Growth Cone Plays a Critical Role in Repulsive Axon Turning

Adrianne L. Kolpak,[1]* Jun Jiang,[1]* Daorong Guo,[1] Clive Standley,[2] Karl Bellve,[2] Kevin Fogarty,[2] and Zheng-Zheng Bao[1]

[1]Department of Medicine and Cell Biology, Program in Neuroscience, and [2]Biomedical Imaging Group, Program in Molecular Medicine, University of Massachusetts Medical School, Worcester, Massachusetts 01605

Macropinocytosis is a type of poorly characterized fluid-phase endocytosis that results in formation of relatively large vesicles. We report that Sonic hedgehog (Shh) protein induces macropinocytosis in the axons through activation of a noncanonical signaling pathway, including Rho GTPase and nonmuscle myosin II. Macropinocytosis induced by Shh is independent of clathrin-mediated endocytosis but dependent on dynamin, myosin II, and Rho GTPase activities. Inhibitors of macropinocytosis also abolished the negative effects of Shh on axonal growth, including growth cone collapse and chemorepulsive axon turning but not turning per se. Conversely, activation of myosin II or treatment of phorbol ester induces macropinocytosis in the axons and elicits growth cone collapse and repulsive axon turning. Furthermore, macropinocytosis is also induced by ephrin-A2, and inhibition of dynamin abolished repulsive axon turning induced by ephrin-A2. Macropinocytosis can be induced *ex vivo* by high Shh, correlating with axon retraction. These results demonstrate that macropinocytosis-mediated membrane trafficking is an important cellular mechanism involved in axon chemorepulsion induced by negative guidance factors.

Introduction

Macropinocytosis is a type of fluid-phase endocytosis characterized by its independence of clathrin and formation of relatively large-sized vesicles, with diameters ranging from 0.2 to 1 μm (Swanson and Watts, 1995; Conner and Schmid, 2003; Porat-Shliom et al., 2008). Generally poorly characterized with few specific markers, macropinocytosis has been shown to be important for fluid and nutrient uptake in *Dictyostellium* (Maniak, 2001) and immune surveillance in dendritic cells (Nobes and Marsh, 2000). In other types of cells, macropinocytosis occurs at a low spontaneous rate but is rapidly induced in response to growth factors. The function of macropinocytosis in the cells outside of the immune system remains elusive.

In response to growth factor stimulation, membrane ruffles are generated through localized actin filament assembly, which can subsequently close into macropinosomes (Swanson, 2008). In macrophages, nonmuscle myosin II-based contractile activity has been shown to be required to curve ruffles into macropinosomes (Araki et al., 2003). Dynamin is a large GTPase involved in budding and scission of nascent vesicles from membranes. Decreasing dynamin 2 activity by expressing a dominant-negative construct or small interfering RNA transfection has been shown to inhibit macropinocytosis (Schlunck et al., 2004; Cao et al., 2007).

Many diffusible protein factors have been identified that exert positive or negative effects on axon growth and guidance (Tessier-Lavigne and Goodman, 1996; Flanagan and Vanderhaeghen, 1998; Song and Poo, 1999). When applied asymmetrically to the growth cones, negative guidance factors induce chemorepulsive turning to steer axons away from the factor. When added in bath, negative guidance molecules cause rapid collapse of growth cones characterized by a loss of lamellipodia and filopodia, followed by axon retraction (Luo and O'Leary, 2005). In contrast, positive guidance factors induce attractive turning and stimulate axon growth. However, molecular and cellular mechanisms underlying the effects of guidance factors are still fragmentary. In response to soluble repellents such as Sema3A and ephrin-A2, a significant increase in dextran-accumulating macropinosomes has been reported (Fournier et al., 2000; Jurney et al., 2002). However, the dextran-positive (dex^+) macropinocytic vesicles in the axons remain poorly characterized, and their function has not been clearly demonstrated. Interestingly, an increase in dextran uptake has also been reported in dystrophic growth cones of dorsal root ganglion neurons *in vitro* and adult nerve endings after spinal cord injury (Tom et al., 2004).

We showed previously that the Sonic hedgehog (Shh) protein has concentration-dependent effects on the growth of retinal ganglion cell (RGC) axons, acting as a positive factor at lower concentrations and a negative factor at higher concentrations (Kolpak et al., 2005). Shh regulates axonal growth in a rapid, transcription-independent manner that requires the activity of its seven transmembrane coreceptor, Smoothened (Smo) (Trousse et al., 2001; Charron et al., 2003; Kolpak et al., 2005). However, the signaling mechanisms underlying the effects of Shh on RGC ax-

Received May 19, 2009; revised July 3, 2009; accepted July 15, 2009.

This work was supported by National Institutes of Health Grant EY014980 (Z.-Z.B.) and Predoctoral Fellowship FNS058170A (A.L.K.). We thank Drs. Yi Rao (Beijing University, Beijing, China) and Jane Wu (Northwestern University, Evanston, IL) for providing Slit2 constructs and Dimitra Efthymiadis, Richard Tuft, and Changan Guo for their participation in the initial stages of the study.

*A.L.K. and J.J. contributed equally to the work.

Correspondence should be addressed to Zheng-Zheng Bao, Department of Medicine and Cell Biology, Program in Neuroscience, University of Massachusetts Medical School, Worcester, MA 01605. E-mail: zheng.bao@umassmed.edu.

DOI:10.1523/JNEUROSCI.2355-09.2009

 0270-6474/09/2910488-11$15.00/0

onal growth remain unclear. Here, we show that high concentration of Shh (high Shh) activates Rho GTPase and nonmuscle myosin II and induces macropinocytosis in the growth cones of RGC axons. We provide evidence that macropinocytosis-mediated membrane trafficking is essential for chemorepulsion induced by negative guidance factors.

Materials and Methods

RGC axon culture and time-lapse microscopy. For RGC axon cultures, embryonic day 6 (E6) chick retinas were dissected, mounted on nitrocellulose filters, and cut into 300-μm-wide strips. Retinal strips were then mounted vitreal side down on glass coverslips. Glass coverslips were coated with 20 μg/ml poly-D-lysine (Sigma), followed by coating with 1.5–10 μg/ml laminin (BD Biosciences and Invitrogen) to achieve consistent axonal growth patterns and dextran uptake. The retinal explants were cultured for 19–22 h in F-12 media containing 0.4% methyl cellulose (Sigma) and penicillin/streptomycin.

Time-lapse experiments were performed on a Carl Zeiss Axiovert 200 microscope with a 10× Plan Neofluar objective. RGC axon cultures were maintained in culture media on a heated microscope stage. Growth cone collapse was scored by a loss of lamellipodia and filopodia to less than three per axon. Three to five independent sets of experiments were performed to determine the rate of growth cone collapse. *Ex vivo* time-lapse microscopy was performed essentially as described previously (Brittis et al., 1995). E6 retina was whole mounted on nitrocellulose filters and incubated with DiI crystals for 2 h at 37°C in DMEM–F-12 media with 10% FBS. Time-lapse microscopy was performed on a heated microscope stage, and filming started immediately after addition of vehicle control or 4.0 μg/ml Shh.

Retinal dissociation and transferrin uptake. E6 chick retina was harvested and incubated in trypsin–EDTA for 8 min at 37°C. Trypsinization was stopped by adding 10% FBS in DMEM, and cells were collected by centrifugation at 1200 rpm for 5 min. The dissociated retinal cells were cultured on poly-D-lysine and laminin-coated coverslips in F-12–0.4% methylcellulose media overnight. The next day, cells were pretreated with vehicle control or 10 μM monodansyl cadaverine (MDC) for 15 min before addition of 20 μg/ml FITC-conjugated transferrin for 5 min at 37°C. Cells were washed twice with ice-cold PBS and fixed with 4% paraformaldehyde.

Dextran internalization. A total of 2.5 mg/ml 10,000 FITC–dextran (Invitrogen) was added to RGC axon cultures. Recombinant mouse Shh-N protein (R & D systems) was used at 2.5–3.5 μg/ml as a high concentration or 0.5 μg/ml as a low concentration. Slit2-conditioned supernatant was prepared by transfection of human embryonic kidney HEK 293T cells with an expression construct encoding the human Slit2 protein (gift from Dr. Yi Rao and Dr. Jane Wu). Supernatant was used straight without dilution. Cyclopamine at 2.5 μM (Toronto Research Chemicals) was added 30 min before dextran addition. The effects of cytochalasin D (Sigma), jasplakinolide (Invitrogen), dynasore (Tocris Bioscience), myristoylated dynamin inhibitory peptide (Tocris Bioscience), blebbistatin (Toronto Research Chemicals), C3 transferase (Cytoskeleton), LY294002 [2-(4-morpholinyl)-8-phenyl-1(4*H*)-benzopyran-4-one] (Calbiochem), chlorpromazine (Sigma), and MDC (Sigma) on dextran uptake were assayed by pretreating the RGC axons with 80 μM dynasore for 3 min, 10 μM MDC, 40 nM jasplakinolide, 100 μM blebbistatin, or 10 μM cytochalasin D for 5 min, 1 μg/ml C3 transferase for 2 h, 25 μM LY294002 for 30 min, and 50 μM myristoylated dynamin inhibitory peptide or 20 μg/ml chlorpromazine for 45 min, before addition of dextran for an additional 2 min at 37°C.

After labeling, axons were washed and fixed in 4% paraformaldehyde. Fluorescence and differential interference contrast (DIC) images were acquired using a 63× Plan Apochromat objective on an inverted Carl Zeiss Axiovert 200 microscope. The percentage of dex^+ axons was scored from ~100 randomly chosen RGC axons for each sample, and a total of three to five sets of independent experiments were performed. Only the axons that could be clearly identified were scored. In the case that the axons were tangled, the whole group was excluded from the data. The dextran-positive signals were verified with the DIC image to confirm that they were in the reverse shadow-cast or protrusive vesicles. Some key data presented in this manuscript have been independently verified by different investigators. Control experiments were performed in parallel of all the experiments for normalization of the data and to ensure consistency of the results.

Immunofluorescence staining. RGC axons were fixed with 4% paraformaldehyde for 20 min and then blocked with 10% calf serum and 0.1% Triton X-100 in PBS. Primary antibodies used were as follows: anti-clathrin heavy chain (Transduction Labs), anti-Smo (MBL International), anti-phospho-myosin light chain (Abcam), anti-hemagglutinin (HA) (Roche), anti-myosin IIA (Covance), anti-myosin IIB (Developmental Studies Hybridoma Bank), and anti-Shh and anti-Rab34 (Santa Cruz Biotechnology). Antibody staining of the dextran-labeled samples was performed by fixation with 4% paraformaldehyde for 2 h, followed by permeabilization with 0.01% Triton X-100 for 1 min or 10 min with methanol at −20°C. Incubation with primary and secondary antibodies was performed as usual. For staining dextran-labeled axons with Alexa 594-conjugated phalloidin, retinal cultures were fixed with 4% paraformaldehyde for 2 h, permeabilized with 0.01% Triton X-100 for 1 min, and then blocked with 1% BSA for 30 min. Alexa 594-conjugated phalloidin (Invitrogen) was diluted in PBS (1:100) and incubated for 2 h at room temperature. Stained samples were analyzed using the Leica TBS SP2 confocal microscope and software.

Axon turning assay and stripe assay. RGC axons were cultured on glass-bottom dishes precoated with poly-D-lysine and laminin for 16–20 h. HEPES buffer was added to the dish before placing onto the stage of a microscope (Olympus U-TB190) enclosed in a 37°C heated chamber. A custom software was generated to control the picospritzer to apply positive pressure to the pipette at a frequency of 2 Hz and a pulse duration of 2 ms. A micromanipulator was used to position the pipette at an angle of 45° from the initial direction of axonal extension. The pipette tip was positioned at ~150 μm distance from the growth cone, and time-lapse movies were produced to record the movement of the growth cone for 30 min. Vehicle control or 3.5 μg/ml Shh protein was loaded in the capillary pipette as control or high Shh, respectively. Before the application of protein from micropipette, axons were pretreated by addition of the following inhibitors to the media: 100 μM blebbistatin for 5 min, 80 μM dynasore for 5 min, 10 μM MDC for 5 min, and C3 transferase for 30 min.

Data were analyzed similarly as published previously (Lohof et al., 1992; Zheng et al., 1994, 1996). The positions of the growth cone centers were marked throughout the time course of the gradient application. Only axons that extended >5 μm in the period of 20 min were included in the analysis. The turning angle α° was determined as the angle of the original direction of axon extension and a line connecting the positions of growth cones at the beginning and the end of gradient application. The lengths of axon extension were calculated by the neurite lengths at the end time point (L_t) subtracting the length at the beginning (L_0) and converted to micrometers based on the scale bar.

FM1-43 [*N*-(3-triethylammoniumpropyl)-4-(4-(dibutylamino)styryl) pyridinium dibromide] labeling was performed by adding the dye at the concentration of 2.5 μM to the RGC axon culture. High Shh (3.5 μg/ml) was provided from one side of the growth cones through a micropipette controlled by picospritzer. Fluorescent images of FM1-43 dye were recorded using a 60× objective lens at a frequency of 5 s/frame and for a duration of 10 min. Growth cones were divided into two halves at the midlines of the last 20 μm segment of the axon, one half facing the micropipette and the other half facing away. Vesicles larger than 0.2 μm diameter formed in the two halves during the 10 min of high Shh application were scored.

Transfection of dominant-negative dynamin constructs (American Type Culture Collection) was performed by electroporation of retinal explants using a square-wave electroporator CUY-21 (Nepa Gene Company), before setting up stripe cultures. Retinal tissues were submerged in 0.1 mg/ml DNA solution, and three pulses of 50 ms duration each at 10 V were applied. Stripe assay was performed similarly as in our previous study (Kolpak et al., 2005).

Western blot. E6 retina were harvested, starved for 15–30 min, and then treated with 0.1% BSA or 3.0 μg/ml Shh for 2 min. Retina were washed twice with ice-cold PBS and lysed, and then Western blots were per-

formed. Rho and Rac activity were assayed using the Rho and Rac activation kits, respectively, according to the instructions of the manufacturer (Upstate). For phospho-myosin light chain experiments, retina were lysed and blotted with phosphor-myosin light chain (1:5000; Abcam) or α-tubulin (1:1000; Sigma) primary antibodies, followed by peroxidase-conjugated secondary antibodies (1:10,000; Jackson ImmunoResearch). Western blots were developed using ECL detection reagents (Pierce).

Statistical analysis. All data are expressed as mean ± SEM. Statistical analyses were performed using the ANOVA test for comparison of multiple samples, followed by Student's *t* test to compare individual samples with the control. *p* values <0.05 were considered to be statistically significant.

Results

High concentration of Shh induces macropinocytosis

The RGC axons were labeled for 15 min with a macropinocytosis marker, FITC–dextran. Dextran labeling was found in endocytic vesicles in a subset of untreated or control vehicle-treated axons (Fig. 1*A*). Most of the vesicles appeared round (0.2–1.0 μm diameter), whereas some appeared as elongated tubules (2–5 μm long) (data not shown). These dex$^+$ vesicles corresponded to visible structures in DIC microscopy images mostly as "reverse shadow-cast" vesicles and occasionally as "protrusive" vesicles in the axonal growth cones and shafts (Fig. 1*A*), similar to that reported previously (Fournier et al., 2000).

Incubation of FITC–dextran with a negative factor, a high concentration of Shh (2.5 μg/ml) (Kolpak et al., 2005), for 15 min significantly increased the percentage of dex$^+$ axons (70.7 ± 3.1%, mean ± SEM) compared with the vehicle control (46.0 ± 1.2%; $p < 0.001$) (Fig. 1*A*,*B*). The number of vesicles per axon also appeared increased by a high concentration of Shh. The growth cones of the dex$^+$ axons in the Shh-treated samples were essentially collapsed, defined by a loss of lamellipodia and a decrease of the number of filopodia to fewer than three per axon. A total of 72.8 ± 2.1% of the dex$^+$ axons showed collapsed growth cones ($n = 169$ axons). Another negative guidance factor to the RGC axons, Slit2, caused a similar increase in dextran labeling correlating with growth cone collapse (Fig. 1*B*, and data not shown). Cyclopamine, a specific inhibitor of Shh signaling (Chen et al., 2002), abolished the effects of high concentrations of Shh on dextran labeling (Fig. 1*B*), suggesting that this effect is specific to the Shh signaling pathway.

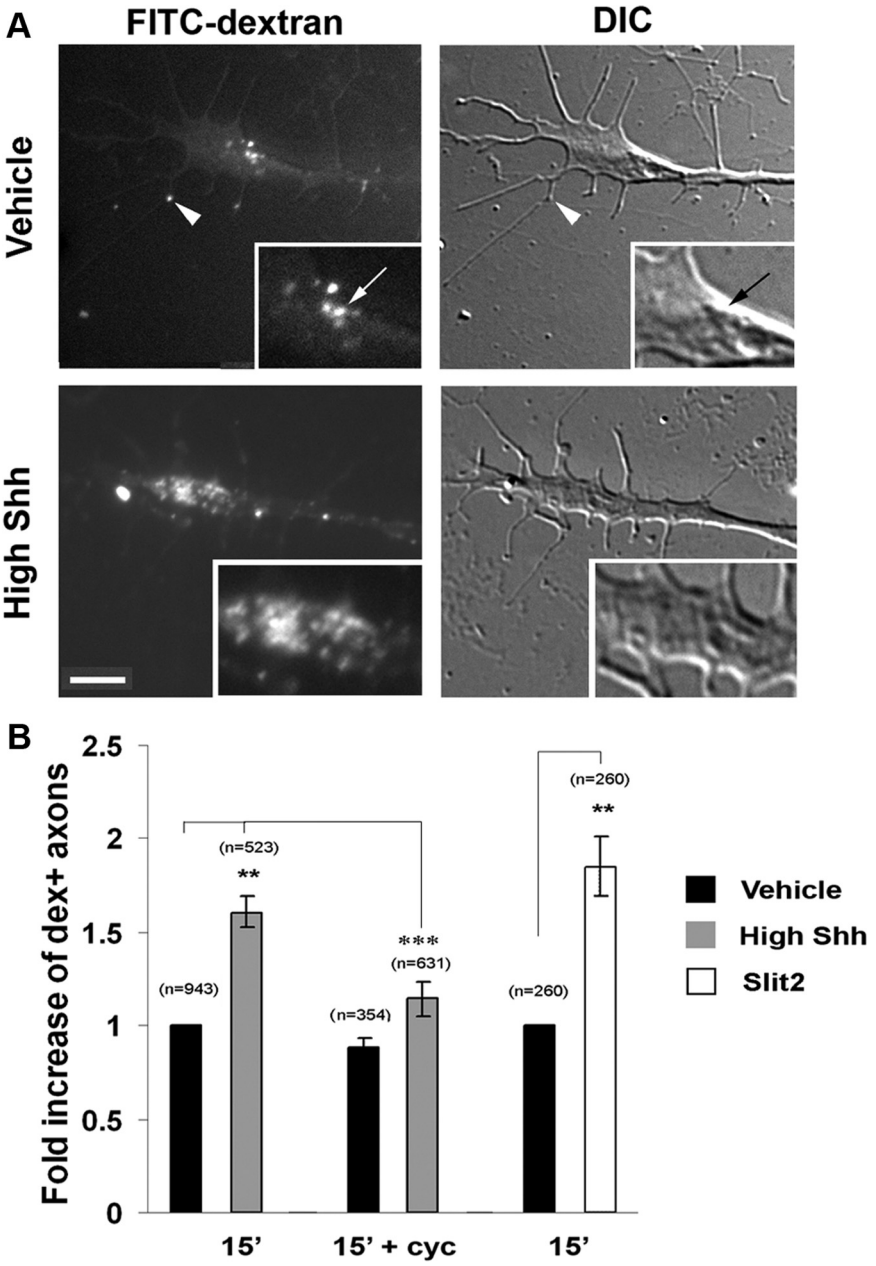

Figure 1. A high concentration of Shh increases dextran$^+$ vesicles in RGC axons. ***A***, RGC axons were labeled with FITC– dextran for 15 min, with vehicle control, high Shh, or Slit2. The dex$^+$ vesicles correspond to visible structures in DIC images, including reverse shadow-cast vesicles (arrow, inset), or protrusive vesicles (arrowhead). The insets are a twofold enlargement of the images. Scale bar, 5 μm. ***B***, The percentages of dextran-positive axons were quantified and normalized to control. An inhibitor of Shh signaling, cyclopamine (cyc), abolished the effects of high concentrations of Shh on dextran labeling. $^{**}p < 0.01$, $^{***}p < 0.001$, Student's *t* test. Numbers in parentheses indicate the total number of axons scored.

The dex$^+$ vesicles are independent of clathrin and mostly unassociated with Shh or Smoothened proteins

By 2 min pulse labeling instead of 15 min labeling of dextran, most of the dex$^+$ vesicles were found to localize to the growth cones (87.2 ± 0.7%) (supplemental Fig. 1*A*, available at www.jneurosci.org as supplemental material). A 15 min chase in the culture media resulted in a shift of localization of the dex$^+$ vesicles to the shaft (38.6 ± 1.9% in the growth cones), suggesting that dextran uptake occurs rapidly and predominantly in the growth cone and that some of the dex$^+$ vesicles are transported retrogradely toward the cell body. A similar increase in dextran uptake by high Shh using 2 min pulse labeling was also observed, confirming that high Shh increases dextran uptake (see Figs. 4*C*, 6*C*) (supplemental Fig. 1*B*,*C*, available at www.jneurosci.org as supplemental material). The 2 min pulse labeling was used for all subsequent experiments to allow characterization of nascent ves-

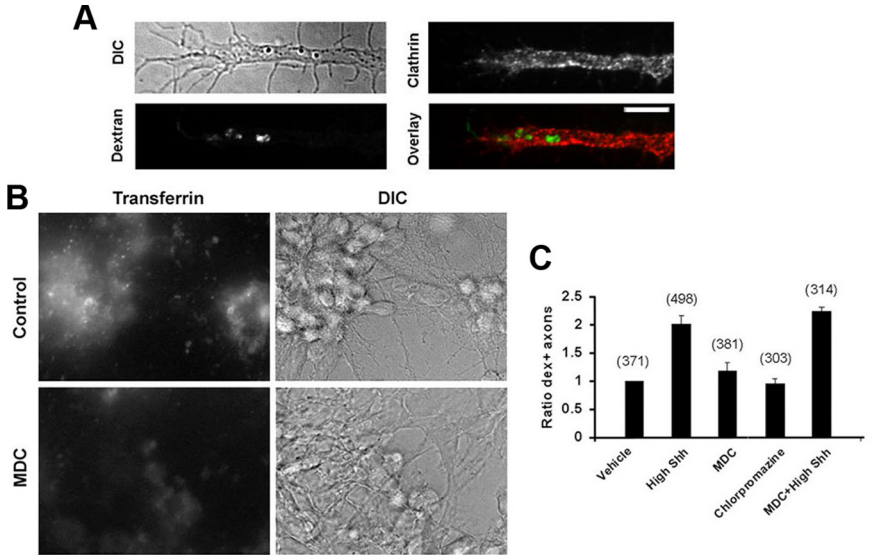

Figure 2. The dex$^+$ vesicles are independent of clathrin. ***A***, RGC axons were labeled with dextran, followed by staining with an anti-clathrin heavy chain antibody. Clathrin-positive puncta appeared excluded from the dex$^+$ vesicles. ***B***, An inhibitor to clathrin-mediated endocytosis, MDC, inhibited transferrin uptake in the cultured retinal cells via clathrin-dependent vesicles. ***C***, MDC did not inhibit dextran uptake induced by high Shh or in the basal condition. Another inhibitor of clathrin-mediated endocytosis, chlorpromazine, also did not inhibit dextran uptake.

icles as confirmed by the absence of the early endosome marker EEA-1 (data not shown) rather than vesicles downstream in the pathway.

The average diameter of the dex$^+$ vesicles was measured to be ~0.4 μm, which is in the range for macropinosomes and substantially larger than the 0.1 μm average diameter of clathrin-coated vesicles. Macropinosomes are poorly characterized endocytic vesicles and have few definitive markers. Antibody staining of clathrin heavy chain did not appear to associate with the dex$^+$ vesicles (Fig. 2*A*). An inhibitor of clathrin-mediated endocytosis, MDC (Ray and Samanta, 1996; Piper et al., 2006), inhibited transferrin uptake via clathrin-mediated vesicles but did not affect dextran uptake in either the untreated control or high concentration of Shh-treated samples (Fig. 2*B*,*C*). Similarly, another inhibitor to clathrin-mediated endocytosis, chlorpromazine, did not inhibit dextran uptake in the RGC axons (Fig. 2*C*), suggesting that the dex$^+$ vesicles are independent of clathrin.

The distributions of Shh and the coreceptor Smo proteins were compared with the dex$^+$ vesicles. RGC cultures treated with high concentration of Shh and FITC–dextran for 5 min were stained by an anti-Shh antibody. The dex$^+$ vesicles did not appear to associate closely with the Shh protein (supplemental Fig. 2*A*, available at www.jneurosci.org as supplemental material), neither was Smo concentrated on the dex$^+$ vesicles (supplemental Fig. 2*B*, available at www.jneurosci.org as supplemental material) in the presence or absence of Shh. These results suggest that the dex$^+$ vesicles are not the main vesicles to mediate trafficking of the Shh or Smo proteins.

Dynamic filamentous actin and nonmuscle myosin II activity are required for macropinocytosis in the axons

To characterize the macropinocytosis in the axons, we examined the regulators known to affect macropinocytosis in non-neuronal cells. Filamentous actin (F-actin) has been shown to transiently surround macropinosomes in *Dictyostellium* (Lee and Knecht, 2002), and F-actin assembly is required for membrane ruffles and macropinocytosis (Swanson, 2008). In control RGC cultures, a majority of the F-actin was organized in filopodia and lamellipodia in the growth cones (supplemental Fig. 3, available at www.jneurosci.org as supplemental material). High Shh caused a rapid reorganization of the actin cytoskeleton, with increasing amounts of F-actin surrounding the reverse shadow-cast dex$^+$ vesicles (Fig. 3*A*) (supplemental Fig. 3, available at www.jneurosci.org as supplemental material). Disassembly of actin filaments by cytochalasin D or latrunculin, or inhibition of F-actin dynamics by jasplakinolide, significantly reduced dextran uptake compared with the vehicle control (Fig. 3*C*, and data not shown).

In macrophages, an inhibitor to myosin light chain kinase, ML-7, was used to show that inhibition of myosin II attenuated macropinocytosis (Araki et al., 2003). By immunofluorescent staining, myosin IIA was shown to localize throughout the RGC axons, whereas myosin IIB was concentrated in the growth cones, particularly around some dex$^+$ vesicles (Fig. 3*B*). A specific inhibitor to myosin II, blebbistatin, effectively inhibited dextran uptake in both the control and high Shh-treated samples (Fig. 3*C*). In non-neuronal cells, macropinocytosis has been shown to require the activity of phosphoinositide 3-kinase (PI3K) (Amyere et al., 2002). However, inhibition of PI3K activity using the pharmacological inhibitors LY294002 or wortmannin did not affect dextran uptake in RGC axons induced by high Shh or under control conditions (Fig. 3*C*). These results suggest that macropinocytosis in the axons share common characteristics with macropinocytosis in non-neuronal cells but also have distinct features.

Inhibitors to macropinocytosis inhibits growth cone collapse induced by high concentration of Shh

The negative effect of high Shh on RGC axon growth was further characterized by time-lapse microscopy. As shown in Figure 4*A* and supplemental Video 1 (available at www.jneurosci.org as supplemental material), high Shh caused rapid growth cone collapse in the RGC axon culture, followed by axon retraction. To determine whether Shh-induced macropinocytosis plays a role in these negative effects on axonal growth, various inhibitors were tested for their effects on growth cone morphology by using time-lapse microscopy. Cytochalasin D collapsed nearly all the growth cones but inhibited axon retraction with or without the presence of high Shh (data not shown), whereas jasplakinolide inhibited growth cone collapse but caused the axon core domain to retract (supplemental Fig. 4*A*, available at www.jneurosci.org as supplemental material). Actin dynamics is thus important for growth cone collapse, precluding the use of these reagents in the experiments of high Shh-induced growth cone collapse.

Treatment of the RGC axons with the inhibitor of nonmuscle myosin II, blebbistatin, did not cause visible growth cone abnormality when added alone but completely abolished high Shh-induced growth cone collapse and axon retraction (Fig. 4*A*,*B*). In contrast, inhibitors of clathrin-mediated endocytosis (MDC) or PI3K (LY294002) did not have significant effect on growth cone

collapse or axon retraction induced by high Shh or in the control condition (Fig. 4*B*). The effects of these inhibitors on growth cone collapse appear to correlate well with their effects on dextran uptake in the RGC axons.

Myosin II activity requires phosphorylation of regulatory myosin light chain, which is subject to regulation by myosin light chain kinase, Rho kinase, and myosin light chain phosphatase (Matsumura, 2005). To determine whether high concentration of Shh increases the activity of nonmuscle myosin II, we examined the level of phosphorylated myosin II light chain by Western blot and immunofluorescent staining. As shown in Figure 4, *C* and *D*, 2 min treatment of high concentration of Shh significantly increased the level of phosphorylated myosin II light chain in the growth cone compared with vehicle control. The mean fluorescent intensity of the staining in high Shh-treated samples was measured at 18.2 ± 0.6 arbitrary units ($n = 80$ axons) versus 12.1 ± 0.7 in vehicle-treated samples ($n = 60$ axons). By using the RBD domain of Rhotekin in pull-down experiments, 5 min treatment of high Shh was found to markedly increase the level of Rho GTPase but not Rac GTPase activity (Fig. 4*C*). To confirm the involvement of Rho GTPase in high Shh-mediated axon growth effects, Rho GTPase activity was inhibited by a membrane-permeable C3 transferase. C3 transferase abolished the increase of dextran uptake (Fig. 3*C*), as well as growth cone collapse and axon retraction induced by high concentration of Shh (Fig. 4*A*,*B*, and data not shown). These results demonstrate that high Shh activates a noncanonical pathway, including Rho GTPase and nonmuscle myosin II, leading to increased macropinocytosis, growth cone collapse, and axon retraction.

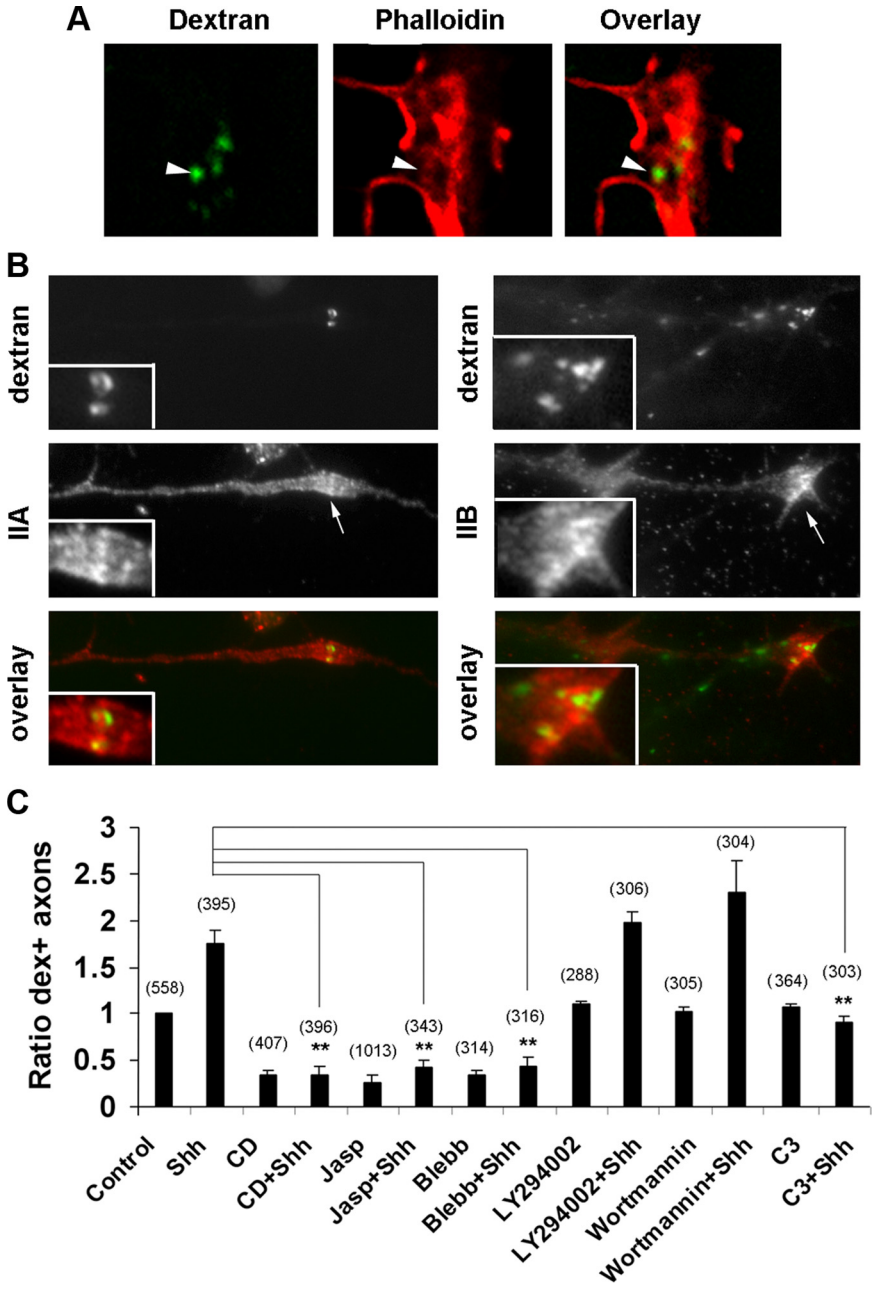

Figure 3. Characterization of the dex$^+$ vesicles in RGC axons. ***A***, RGC axons labeled with high Shh and dextran for 5 min were stained with phalloidin. By confocal microscopy analysis, some dex$^+$ vesicles appeared surrounded by actin filaments (arrowheads). ***B***, RGC axons labeled by dextran in the presence of high Shh were subsequently stained by antibodies specific to myosin IIA and IIB heavy chains. ***C***, RGC axons were pretreated with vehicle control, cytochalasin D (CD), jasplakinolide (Jasp), blebbstatin (Blebb), or LY294002, wortmannin, or C3 transferase before incubation with dextran for 2 min in the presence or absence of high Shh. The percentages of dextran-positive axons were quantified and normalized to the controls. Data are represented as mean ± SEM. $^{**}p < 0.01$, Student's *t* test. Numbers in parentheses indicate the total number of axons scored.

Inhibition of dynamin activity decreases dextran uptake and growth cone collapse

To further characterize the role of macropinocytosis in the negative effects of high concentration of Shh on RGC axons, we analyzed whether dynamin is required for macropinocytosis in the axons. Dynamin is a large GTPase involved in scission of budding vesicles from the plasma membrane and has been shown to be essential for various types of endocytosis (Praefcke and McMahon, 2004). Two different membrane-permeable dynamin inhibitors were used to rapidly inhibit dynamin function. Dynasore, a specific noncompetitive inhibitor of dynamin 1 and 2 (Macia et al., 2006), and a myristoylated dynamin inhibitory peptide, a competitive inhibitor that prevents association of dynamin and amphiphysin (Wigge et al., 1997), were added to the axons, and dextran uptake experiments were performed. Both dynasore and dynamin inhibitory peptide significantly decreased the basal level and high Shh-induced dextran uptake (Fig. 5*C*), suggesting that macropinocytosis in RGC axons requires the function of dynamin.

Time-lapse microscopy was also performed on axons pretreated with dynasore or dynamin inhibitory peptide to assess growth cone collapse and axon retraction under control and high Shh-treated conditions. Treatment with dynasore did not alter growth cone morphology within 10 min compared with control axons but reduced axonal growth rate after a longer period of

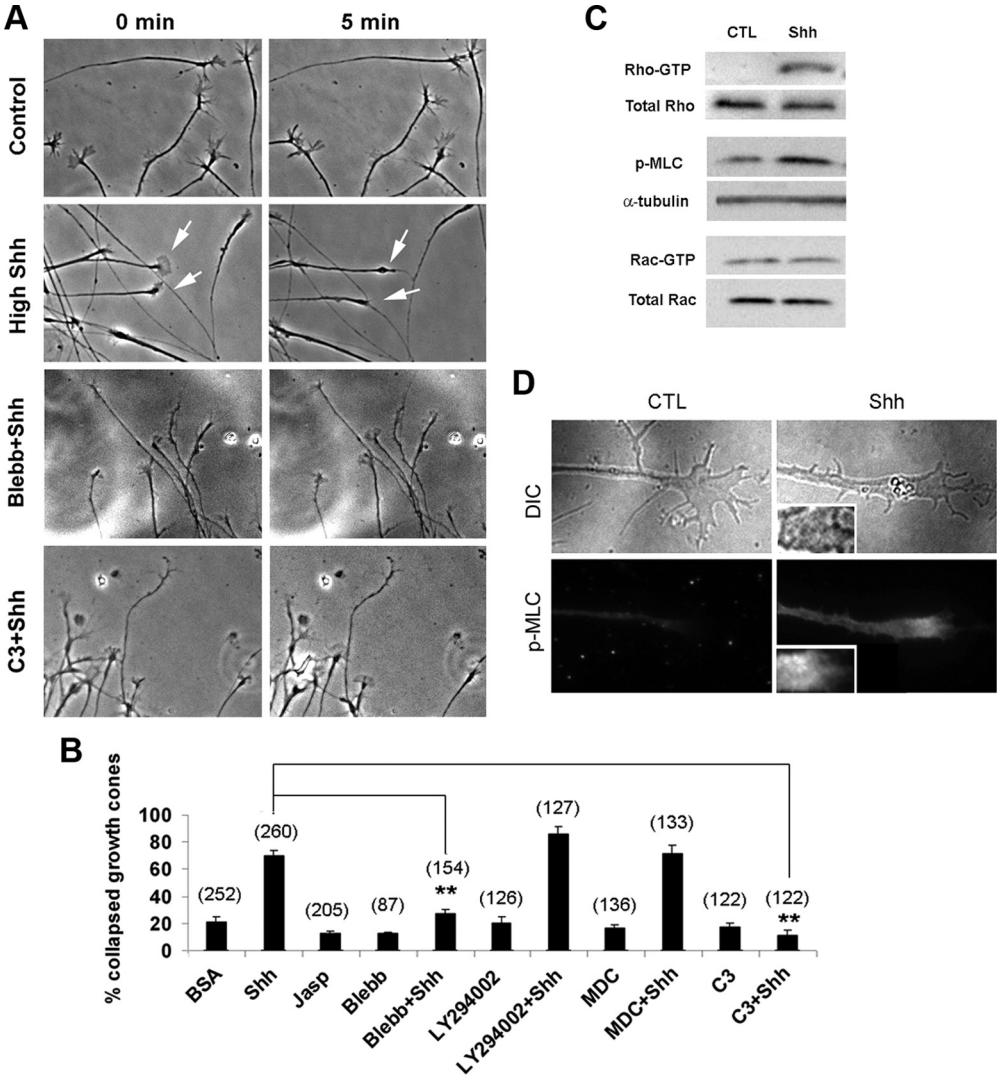

Figure 4. ***A***, Time-lapse microscopy was performed to analyze growth cone collapse in the presence of vehicle control, high Shh or high Shh with blebbistatin, or C3 transferase. Note that blebbistatin and C3 transferase inhibited growth cone collapse in response to high Shh. ***B***, Percentages of growth cone collapse in the presence of various inhibitors were scored. Growth cone collapse was defined as loss of lamellipodia and reduction of filopodia number to less than three per axon. Data are represented as mean ± SEM. $^{**}p < 0.01$, Student's *t* test. Numbers in parentheses indicate the total number of axons scored. ***C***, To analyze the Rho or Rac GTPases activities, cell extracts from the retinal tissues treated with vehicle control or high concentration of Shh for 2 min were immunoprecipitated by RBD domain of Rhotekin or PBD domain of Pak and blotted by anti-Rho or anti-Rac antibodies, respectively. Cell extracts treated with control (CTL) or high Shh for 2 min were also analyzed by Western blot using anti-phospho-myosin light chain antibody. ***D***, Immunofluorescent staining using anti-phospho-myosin light chain antibody was performed in RGC axonal cultures. Insets represent 2× magnification of the images.

incubation. In untreated control cultures, addition of high Shh led to rapid growth cone collapse in 71.1 ± 3.6% of axons within 5 min, followed by axon retraction (Fig. 5*D*) (supplemental Video 1, available at www.jneurosci.org as supplemental material). In contrast, treatment of dynasore markedly reduced growth cone collapse in response to high Shh to the rate of 23.4 ± 2.3% of axons (Fig. 5*D*) (supplemental Fig. 4, available at www.jneurosci.org as supplemental material), whereas the majority of the growth cones remained motile with active filopodia and lamellipodia (supplemental Video 2, available at www.jneurosci.org as supplemental material). Axon retraction induced by high Shh was also abolished by dynasore (supplemental Video 2, available at www.jneurosci.org as supplemental material). However, the dynamin-inhibitory peptide itself caused growth cone collapse, precluding the analysis of its effect on growth cone collapse in response to high Shh. The difference between the two dynamin inhibitors on growth cone morphology is presently unclear.

Asymmetric macropinocytosis in the growth cone and axon repulsive turning

Next, we examined whether macropinocytosis is involved in axon repulsive turning by using an *in vitro* turning assay, a well established assay for studying molecular and cellular mechanisms involved in axon steering and guidance (Zheng et al., 1994, 1996). As shown in Figure 6*A*, a high concentration of Shh applied through a micropipette placed at a 45° angle to the direction of axon extension elicited repulsive axon turning ~10 min after Shh application. The average turning angle by high Shh was calculated to be −27.3° (Fig. 6*C*). In contrast, vehicle control applied through a micropipette did not cause directional turning with an average of turning angle <5°.

To confirm whether macropinocytosis is induced asymmetrically by high Shh applied through the micropipette, we performed time-lapse microscopy by using the styryl FM1-43 dye, taking advantage of the fact that FM1-43 is nearly nonfluorescent

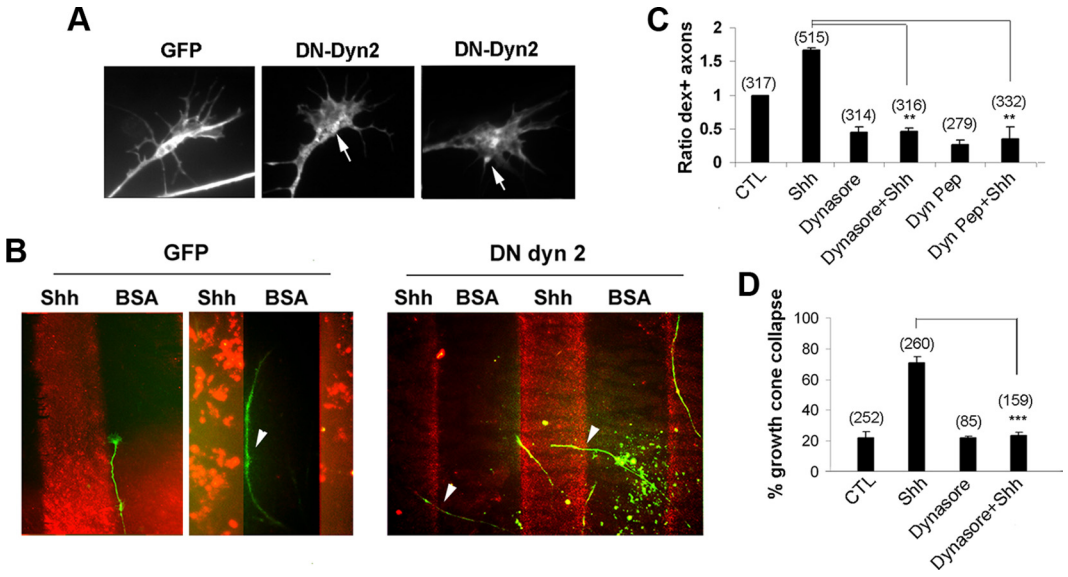

Figure 5. Dynamin is required for dextran uptake and growth cone collapse. ***A***, RGC axons were transfected with constructs expressing GFP or DN dyn2. Note that DN dyn2 appears to surround some large vesicles in the growth cones (arrows). ***B***, Transfected RGCs were tested for their response to high Shh on stripe assay. Note that the GFP-transfected axons mostly turned away from high Shh, whereas DN dyn2-transfected axons ignored the boundary between high Shh/BSA. ***C***, RGC axons were pretreated with vehicle control (CTL), dynasore, dynamin inhibitory peptide (Dyn Pep) before incubation with dextran for 2 min in the presence or absence of high Shh. The percentages of dextran-positive axons were quantified and normalized to the controls. ***D***, Growth cone collapse was scored, and data are represented as mean ± SEM. $^{**}p < 0.01$, $^{***}p < 0.001$, Student's *t* test. Numbers in parentheses indicate the total number of axons scored.

in solution but brightly fluorescent when partitioned into the membrane (Brumback et al., 2004). Colabeling of the RGC axons with FITC-conjugated dextran and FM1-43 showed that FM1-43 brightly labeled macropinosomes, primarily overlapping with the dex$^+$ vesicles (supplemental Fig. 5, available at www.jneurosci.org as supplemental material). Smaller vesicles labeled by FM1-43 were hardly visible, at the level of magnification and exposure time of the camera. A substantially higher number of large FM1-43$^+$ vesicles were observed to form at the side of the micropipette delivering high Shh than the opposing side (69.8 ± 1.5 vs 30.2 ± 1.5%; $n = 115$ vesicles from 10 axons) (Fig. 6*E*). Macropinocytosis thus occurred rapidly at the side of the micropipette providing Shh, before visible axonal turning.

We next determined whether the agents that inhibit macropinocytosis would inhibit repulsive axon turning induced by high Shh. Excluding those inducing growth cone collapse by themselves, inhibitors including dynasore, blebbistatin, and C3 transferase were each added to the culture media, whereas a high concentration of Shh was applied from the micropipette and axonal growth was recorded for a minimum of 20 min. Remarkably, dynasore abolished the repulsive turning induced by Shh, yielding an average turning angle of 1.6° (Fig. 6*B–D*). Similar inhibition of directional turning was observed by blebbistatin and C3 transferase (mean turning angles of 2.2° and −0.8°, respectively). Axons were able to turn in the presence of inhibitors, thus turning per se was not inhibited (Fig. 6*B–D*). Except dynasore, other inhibitors did not appear to significantly affect the lengths of axon extension. Correlating with their lack of effect on macropinocytosis, PI3K inhibitor (LY294002) and the inhibitor of clathrin-mediated endocytosis (MDC) did not affect repulsive turning induced by high Shh (Fig. 6*B–D*).

To confirm that dynamin-mediated macropinocytosis is critical for repulsive turning of RGC axons in response to a high concentration of Shh, we transfected constructs encoding the HA-tagged dominant-negative (DN) forms of dynamin 1 and dynamin 2 (dyn1 K44A and dyn2 K44A) into RGCs (van der Bliek et al., 1993; Sontag et al., 1994). Few axons were found to be positive for DN dyn1. In DN dyn2-transfected RGC axons, DN dyn2 appeared to concentrate around some large vesicles in the growth cones (Fig. 5*A*). Because of technical difficulties, we performed stripe assay instead of turning assay on the transfected axons. After transfection by electroporation, retinal tissues were cultured on glass coverslips coated with alternating stripes of high Shh and BSA. As shown in Figure 5*B*, 90.9% green fluorescent protein (GFP)-transfected axons turned away from high Shh-coated stripes (10 of 11 axons), in contrast to only 34.6% of DN dyn2-transfected axons ($n = 26$ axons). This result confirms that dynamin-mediated macropinocytosis is required for the negative guidance effect induced by high Shh.

Activation of myosin II or phorbol myristate acetate treatment increases macropinocytosis and elicits negative effects on axons

Calyculin A at low concentrations has been shown to specifically inhibit myosin light chain phosphatase (Gupton and Waterman-Storer, 2006), thus enhancing myosin II activity. Treatment of a low concentration of calyculin A significantly increased dextran uptake in the RGC axons (Fig. 7*A*), supporting that myosin II activity is important for macropinocytosis in the RGC axons. Consistent with the notion that macropinocytosis is critical for the effects induced by negative guidance factors, calyculin A induced growth cone collapse when applied in bath (79.0 ± 3.6%; $n = 115$ axons) and repulsive axon turning in turning assay (Fig. 7*B*). Similarly as in macrophages and dorsal root ganglion axons (Swanson, 1989; Fournier et al., 2000), phorbol myristate acetate (PMA) also increased macropinocytosis in the RGC axons (Fig. 7*A*). Accordingly, PMA caused a significant increase in growth cone collapse when added in bath (86.3 ± 5.1%; $n = 155$ axons) and induced repulsive turning in the axon turning assay (Fig. 7*B*). These results demonstrate that increased macropinocytosis by calyculin A and PMA correlates with an increase of negative effects on RGC axons, including growth cone collapse and repulsive axon turning.

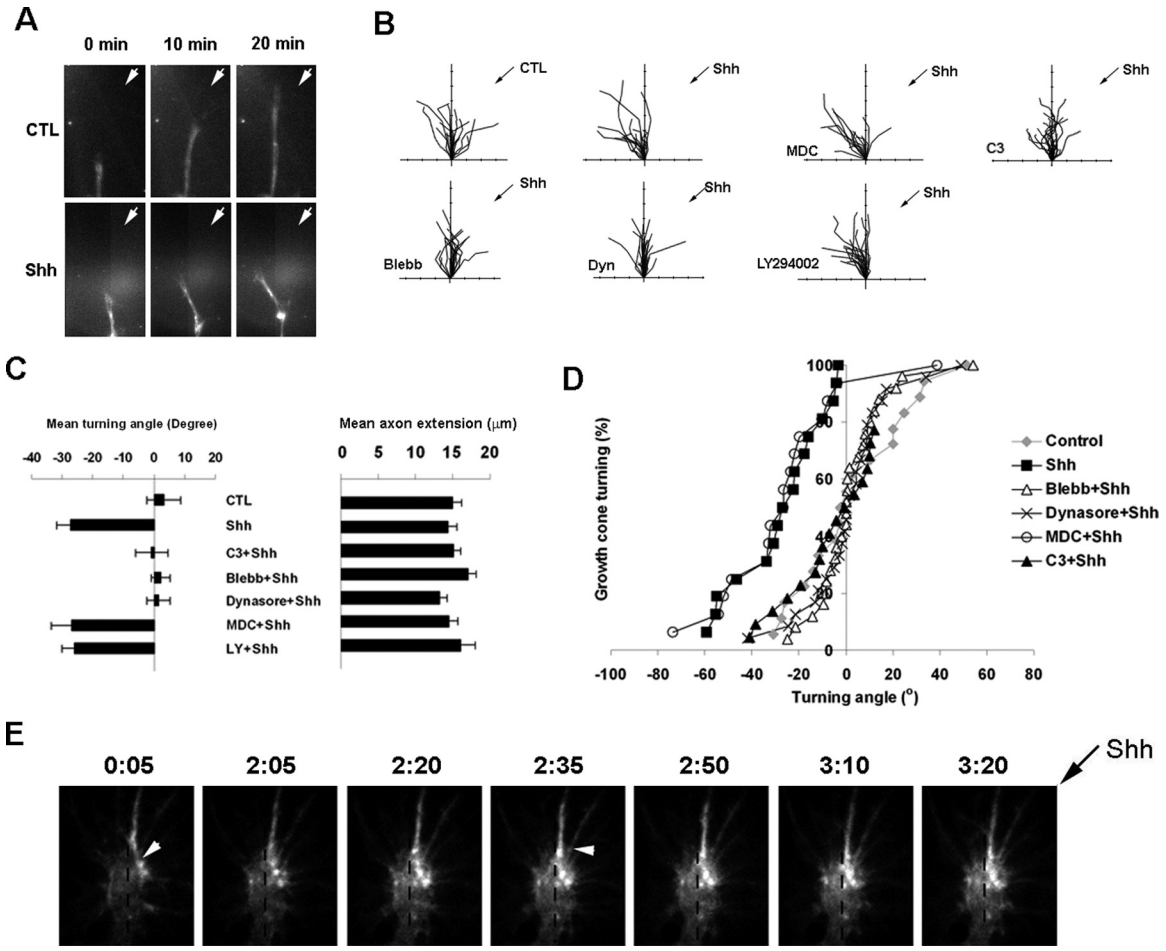

Figure 6. Macropinocytosis is important for chemorepulsive axon turning. ***A***, Turning assay was performed by providing vehicle control (CTL) or high Shh through a micropipette at 45° angle to the direction of axon extension (arrows). ***B***, Composite drawings of the paths of axonal extension during the 20 min filming with various inhibitors in the culture media and high Shh or vehicle control provided via the micropipette (arrows). The origin represents the position of the center of the growth cone at the beginning of recording. The original direction of neurite extension, as defined by the last 20 μm segment of the axonal shaft at the beginning of the experiment, was aligned with the vertical scale line. Tick marks along the *x*- and *y*-axis represent 5 μm. ***C***, Average turning angles and length of net axon extension for each condition are shown. ***D***, Cumulative distributions of turning angles summarize the effects of various inhibitors on the repulsive turning of the RGC axons in response to high Shh. Each point depicts the percentage of growth cones bearing a turning angle equal to or less than the value indicated on the *x*-axis. Positive angles indicate turning toward the pipette, whereas negative angles indicate turning away from the pipette. ***E***, FM1-43$^+$ vesicles (arrowheads) were imaged by fluorescence time-lapse microscopy while Shh protein was provided through a micropipette positioned at 45° angle to the direction of axon extension (arrow). Blebb, Blebbistatin; LY, LY294002.

We further analyzed whether macropinocytosis is important for repulsive turning induced by other negative factors. Ephrin-A2 has been shown to be a negative factor to RGC axons derived from temporal retina and induced macropinocytosis (Nakamoto, 1996; Jurney et al., 2002). We found that macropinocytosis induced by ephrin-A2 was also inhibited by coaddition of dynasore (Fig. 7*D*). By turning assay, ephrin-A2 caused repulsive turning of temporal RGC axons with a turning angle of −16.5°. Addition of dynasore in bath abolished repulsive turning induced by ephrin-A2 (Fig. 7*E*), suggesting that macropinocytosis-mediated membrane trafficking may play a general role in the negative effects of guidance factors.

Macropinocytosis is also regulated by positive factors and can be induced in RGCs *ex vivo*

The effect of positive factors on macropinocytosis was also analyzed. We tested the effect by a low concentration of Shh, which we showed previously as a positive factor (Kolpak et al., 2005). Low concentration of Shh was added with FITC–dextran for 2 or 15 min, and a significant decrease of dextran uptake was observed (Fig. 7*C*). The decrease of macropinocytosis by low concentration of Shh was abolished by addition of cyclopamine, suggesting that the effect is specific to the Shh pathway. Because soluble laminin has been shown to affect axon growth rate and direction (Cohen et al., 1987; Liesi and Silver, 1988), we tested the effect of soluble laminin on the growth and dextran uptake of chick RGC axons. Addition of soluble laminin in the culture induced very rapid increases in chick RGC axon elongation by time-lapse microscopy (data not shown) and, consistently, a decrease of dextran uptake (Fig. 7*C*). We also applied soluble laminin through a micropipette positioned at a 45° angle to the direction of axon extension. Unlike the negative factor, high Shh (Fig. 6*E*), laminin significantly decreased macropinocytosis, because very few axons contained any FM1-43$^+$ vesicles in the presence of laminin (data not shown). These results indicate that macropinocytosis is induced by negative, not positive, factors in the axons.

Finally, we examined whether RGC axons in *ex vivo* explants can internalize dextran in response to high Shh. At E6, the RGC axons were localized very close to the surface at the ganglion cell side. Retinas were dissected and flat mounted onto nitrocellulose filters with the ganglion cell side facing up. FITC–dextran with vehicle control or high concentration of Shh was incubated with

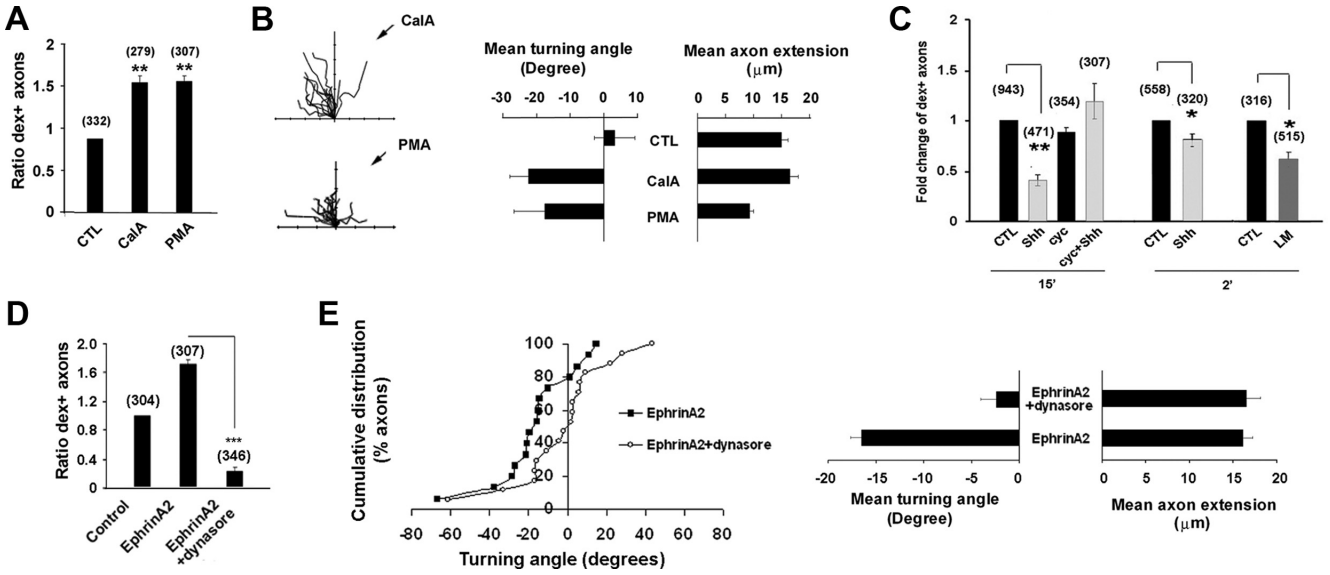

Figure 7. ***A***, Percentages of axons undergoing dextran uptake were scored in the presence of vehicle control (CTL), calyculin A (CalA), and PMA. ***B***, Axon turning assays were performed by providing calyculin A or PMA through a micropipette positioned at 45° angle to the direction of axon extension (arrow). ***C***, RGC axons were treated with vehicle control or low concentration of Shh (0.5 μg/ml) for 2 or 15 min in the absence or presence of cyclopamine (cyc). Percentages of axons positive for dextran were scored and normalize to control. Soluble laminin was also tested for its effect on dextran uptake. Note that both low Shh and laminin (LM) significantly decrease dextran uptake in the RGC axons. ***D***, Macropinocytosis is also required for ephrin-A2-induced repulsive axon turning. Increase of dextran uptake by ephrin-A2 in the RGC axons is significantly inhibited by coaddition of dynasore ($p < 0.001$). ***E***, Turning assay was performed by applying ephrin-A2 through the micropipette. Note that repulsive axon turning induced by ephrin-A2 was abolished by addition of dynasore in bath. Data are represented as mean ± SEM. *$p < 0.05$, **$p < 0.01$, Student's *t* test. Numbers in parentheses indicate the total number of axons scored.

the flat-mount retinal tissues for 2 min at 37°C. The tissues were then washed and fixed. A marked increase of dextran labeling was observed in the RGC layer in the samples treated with high Shh compared with those treated with vehicle control (Fig. 8*A*). To determine whether the increase in dextran uptake correlates with a change in RGC axon growth, RGC axons in the living retinal explants were labeled by DiI following a previously described procedure (Brittis et al., 1995). The movement of ganglion cell growth cones was filmed by fluorescence time-lapse microscopy for 30 min, with the addition of vehicle control or high concentration of Shh in the culture media. Only a small fraction of RGC axons (2 of 28 axons) retracted in the control cultures, in contrast to a much higher proportion of axons (14 of 34 axons) retracted in the high Shh-treated cultures (Fig. 8*B*). These results demonstrate that the negative factor, high Shh, can induce dextran uptake, which correlates with an increase in axon retraction in the living retinal explants, similar to the *in vitro* culture.

Discussion

In this study, we demonstrate that Shh protein induces macropinocytosis in the axons, through activation of a noncanonical signaling pathway. Rho GTPase and nonmuscle myosin II activities were rapidly increased during the treatment of Shh. Macropinocytosis induced by Shh was observed to occur rapidly in the growth cones and was further characterized as independent of clathrin and PI3K but dependent on dynamin and myosin II activities. Inhibitors of macropinocytosis abolished growth cone collapse and repulsive axon turning induced by high Shh, and pharmacologically increased macropinocytosis correlated with growth cone collapse and axon repulsive turning. These results support that macropinocytosis-mediated membrane trafficking is essential for chemorepulsive axon guidance.

Although the correlation of macropinocytosis and axon growth cone collapse has been reported by previous studies (Fournier et al., 2000; Jurney et al., 2002), our study provides the first functional evidence that macropinocytosis-mediated membrane trafficking is essential for growth cone collapse and repulsive axon turning induced by negative factors. An increase in dextran uptake has also been reported in dystrophic growth cones of dorsal root ganglion neurons grown on the proteoglycan aggrecan *in vitro* and adult nerve endings after spinal cord injury, correlating with failure of regeneration (Tom et al., 2004). Although it is not clear whether dextran uptake in the dystrophic nerve is a cause or effect of axon dystrophy, it is very interesting that these vesicles can be induced in both the embryonic and adult axons, under the normal developmental and pathological conditions.

Membrane retrieval associated with repulsive axon turning could conceivably be mediated by detachment of plasma membrane rather than endocytosis. However, inhibition of dynamin function by using a pharmacological inhibitor and expression of a dominant-negative dynamin construct inhibits repulsive axon turning, suggesting that endocytosis is required for this process. Because the inhibitor for clathrin-mediated endocytosis, MDC, does not have any effect on repulsive axon turning, clathrin-independent macropinocytosis is thus the main endocytic mechanism involved in the process. We show that asymmetric macropinocytosis occurs very rapidly (<1 min) after the application of repulsive guidance cue, minutes before visible axon turning was observed. The time sequence supports that macropinocytosis is probably a cause rather than an indirect effect of repulsive axon turning. Because negative guidance factors are known to induce changes in cytoskeletal dynamics, it is unclear whether macropinocytosis alone can drive repulsive axon turning. To resolve this issue, a much better understanding of the molecular mechanisms involved in macropinocytosis is necessary. In an attempt to address this issue, we used PMA and calyculin A, both of which are not known to be axon guidance factors but could induce macropinocytosis in the growth cones. Interestingly, both

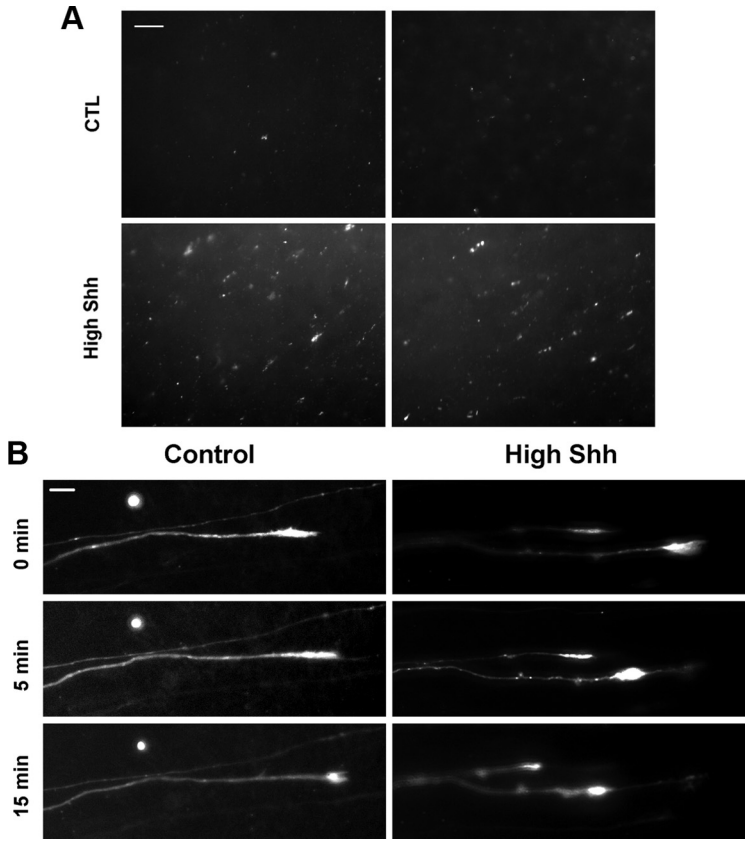

Figure 8. High Shh induces dextran uptake and axon retraction *ex vivo*. ***A***, Dextran uptake can occur *ex vivo* in retinal explants. Flat-mount retinas were incubated with FITC–dextran and vehicle control (CTL) or high Shh for 2 min. The tissues were then washed, fixed, and photographed at the RGC side by fluorescence microscopy. Note that treatment with high Shh induced a marked increase in dextran uptake. ***B***, RGC axons were labeled by DiI in the explant culture. The movement of RGC axons in the explant culture was filmed by time-lapse microscopy in the presence of vehicle control or high Shh in the culture media. Note that high Shh substantially increased the number of axons undergoing retraction compared with the control samples. Scale bars, 10 μm.

PMA and calyculin A caused growth cone collapse and repulsive axon turning, supporting that macropinocytosis plays a crucial role in these processes.

Based on its relatively large size and independence of clathrin, the dex$^+$ vesicles in RGC axons fall into the definition of macropinosomes. Our study demonstrated that macropinocytosis in the axons shares common characteristics with those in non-neuronal cells but with its own distinct features (Swanson and Watts, 1995; Swanson, 2008). Macropinocytosis in axons does not require PI3K, and the dex$^+$ vesicles were also not positive for two macropinosome markers reported in some non-neuronal cells, including Abi-1 and Rab34 (Sun et al., 2003) (data not shown) (supplemental Fig. 6, available at www.jneurosci.org as supplemental material). The independence of PI3K is consistent with the fact that the PI3K pathway generally associates with positive, not negative, axon growth/guidance pathways (Goold et al., 1999).

The requirement of dynamin in macropinocytosis in non-neuronal cells appears to be cell type dependent. In fibroblasts, dominant-negative dynamin 2 inhibits V12Rac- or PDGF-induced macropinocytosis without affecting baseline fluid-phase uptake (Schlunck et al., 2004). Prolonged inhibition of either dynamin 1 or dynamin 2 activities, however, induces a compensatory, dynamin- and clathrin-independent fluid-phase mechanism (Damke et al., 1995; Altschuler et al., 1998). In the RGC axons, inhibitors including dynasore and dynamin inhibitory peptide inhibited high Shh-induced macropinocytosis as well as macropinocytosis in the control cultures without the addition of Shh protein.

Cytochalasin D and dynamin inhibitory peptide inhibit macropinocytosis, consistent with the notion that actin assembly and dynamin are required for macropinocytosis. Cytochalasin D and dynamin inhibitory peptide induce growth cone collapse, suggesting that growth cone collapse can be uncoupled from macropinocytosis under special conditions. However, there is no evidence that macropinocytosis can be uncoupled from repulsive axon turning. Because actin filaments are essentially the only type of cytoskeletal elements present in the filopodia, it is not surprising that depolymerization of actin filaments by cytochalasin D leads to a loss of filopodia, a characteristic of growth cone collapse. In contrast, physiological negative axon guidance factors induce growth cone collapse not through depolymerization but rather reorganization of actin filaments as shown by phalloidin staining (Fig. 3*A*) (supplemental Fig. 3, available at www.jneurosci.org as supplemental material), accompanied with an increase in macropinocytosis. Furthermore, growth cone collapse induced by negative guidance factors, but not those induced by cytochalasin D or dynamin inhibitory peptide, is followed by rapid axon retraction. In fact, cytochalasin D and dynamin inhibitory peptide inhibit axon retraction occurring spontaneously or induced by high Shh (data not shown). Therefore, macropinocytosis appears also to correlate with axon retraction induced by negative factors.

Several studies, including our previous study, demonstrate that Shh regulates axonal growth and guidance in a noncanonical transcription-independent pathway (Trousse et al., 2001; Charron et al., 2003; Kolpak et al., 2005). However, the signaling mechanism underlying the effect of Shh remains unclear. We demonstrate that Shh at high concentration increases activities of Rho GTPase and myosin II. In light of the fact that macropinocytosis is also induced by other negative factors (Fournier et al., 2000; Jurney et al., 2002) and dynasore can inhibit repulsive turning induced by ephrin-A2, macropinocytosis may play a general role in mediating effects of negative guidance factors. Because a low concentration of Shh and soluble laminin decrease macropinocytosis in the axons, macropinocytosis may be a common pathway regulated by both the positive and negative factors.

Because of their large sizes, macropinosomes can be effective in regulating surface protein expression, removing adhesion sites between the growth cone and the substratum, or change the surface area associated with growth cone collapse, axon retraction, and chemorepulsion. When myosin II, Rho, and dynamin activities were inhibited, only the repulsive turning induced by high Shh was abolished but not the turning per se. It is possible that spontaneous turning does not require macropinocytosis of the

same type. Alternatively, exocytosis may contribute to the nondirectional turning in these experiments, as suggested by a recent report that exocytosis is important for supplying membrane during axon growth and attractive axon turning (Tojima et al., 2007). Interestingly, inhibition of VAMP2-mediated exocytosis was reported to only prevent growth cone attraction but not repulsion (Tojima et al., 2007), suggesting that growth cone attraction and repulsion use distinct mechanisms rather than impinging on the same molecular machinery. We present evidence here that macropinocytosis in the growth cone is critical for mediating the effects of negative guidance factors. Therefore, membrane trafficking including endocytosis and exocytosis may emerge as key processes in directional turning of axons induced by axon guidance cues.

References

Altschuler Y, Barbas SM, Terlecky LJ, Tang K, Hardy S, Mostov KE, Schmid SL (1998) Redundant and distinct functions for dynamin-1 and dynamin-2 isoforms. J Cell Biol 143:1871–1881.

Amyere M, Mettlen M, Van Der Smissen P, Platek A, Payrastre B, Veithen A, Courtoy PJ (2002) Origin, originality, functions, subversions and molecular signalling of macropinocytosis. Int J Med Microbiol 291:487–494.

Araki N, Hatae T, Furukawa A, Swanson JA (2003) Phosphoinositide-3-kinase-independent contractile activities associated with Fcgamma-receptor-mediated phagocytosis and macropinocytosis in macrophages. J Cell Sci 116:247–257.

Brittis PA, Lemmon V, Rutishauser U, Silver J (1995) Unique changes of ganglion cell growth cone behavior following cell adhesion molecule perturbations: a time-lapse study of the living retina. Mol Cellular Neurosci 6:433–449.

Brumback AC, Lieber JL, Angleson JK, Betz WJ (2004) Using FM1-43 to study neuropeptide granule dynamics and exocytosis. Methods 33:287–294.

Cao H, Chen J, Awoniyi M, Henley JR, McNiven MA (2007) Dynamin 2 mediates fluid-phase micropinocytosis in epithelial cells. J Cell Sci 120:4167–4177.

Charron F, Stein E, Jeong J, McMahon AP, Tessier-Lavigne M (2003) The morphogen Sonic Hedgehog is an axonal chemoattractant that collaborates with Netrin-1 in midline axon guidance. Cell 113:11–23.

Chen JK, Taipale J, Cooper MK, Beachy PA (2002) Inhibition of Hedgehog signaling by direct binding of cyclopamine to Smoothened. Genes Dev 16:2743–2748.

Cohen J, Burne JF, McKinlay C, Winter J (1987) The role of laminin and the laminin/fibronectin receptor complex in the outgrowth of retinal ganglion cell axons. Dev Biol 122:407–418.

Conner SD, Schmid SL (2003) Regulated portals of entry into the cell. Nature 422:37–44.

Damke H, Baba T, van der Bliek AM, Schmid SL (1995) Clathrin-independent pinocytosis is induced in cells overexpressing a temperature-sensitive mutant of dynamin. J Cell Biol 131:69–80.

Flanagan JG, Vanderhaeghen P (1998) The ephrins and Eph receptors in neural development. Annu Rev Neurosci 21:309–345.

Fournier AE, Nakamura F, Kawamoto S, Goshima Y, Kalb RG, Strittmatter SM (2000) Semaphorin3A enhances endocytosis at sites of receptor-F-actin colocalization during growth cone collapse. J Cell Biol 149:411–422.

Goold RG, Owen R, Gordon-Weeks PR (1999) Glycogen synthase kinase 3beta phosphorylation of microtubule-associated protein 1B regulates the stability of microtubules in growth cones. J Cell Sci 112:3373–3384.

Gupton SL, Waterman-Storer CM (2006) Spatiotemporal feedback between actomyosin and focal-adhesion systems optimizes rapid cell migration. Cell 125:1361–1374.

Jurney WM, Gallo G, Letourneau PC, McLoon SC (2002) Rac1-mediated endocytosis during ephrin-A2- and semaphorin 3A-induced growth cone collapse. J Neurosci 22:6019–6028.

Kolpak A, Zhang J, Bao ZZ (2005) Sonic hedgehog has a dual effect on the growth of retinal ganglion axons depending on its concentration. J Neurosci 25:3432–3441.

Lee E, Knecht DA (2002) Visualization of actin dynamics during macropinocytosis and exocytosis. Traffic 3:186–192.

Liesi P, Silver J (1988) Is astrocyte laminin involved in axon guidance in the mammalian CNS? Dev Biol 130:774–785.

Lohof AM, Quillan M, Dan Y, Poo MM (1992) Asymmetric modulation of cytosolic cAMP activity induces growth cone turning. J Neurosci 12:1253–1261.

Luo L, O'Leary DD (2005) Axon retraction and degeneration in development and disease. Annu Rev Neurosci 28:127–156.

Macia E, Ehrlich M, Massol R, Boucrot E, Brunner C, Kirchhausen T (2006) Dynasore, a cell-permeable inhibitor of dynamin. Dev Cell 10:839–850.

Maniak M (2001) Fluid-phase uptake and transit in axenic Dictyostelium cells. Biochim Biophys Acta 1525:197–204.

Matsumura F (2005) Regulation of myosin II during cytokinesis in higher eukaryotes. Trends Cell Biol 15:371–377.

Nakamoto M, Cheng HJ, Friedman GC, McLaughlin T, Hansen MJ, Yoon CH, O'Leary DD, Flanagan JG (1996) Topographically specific effects of ELF-1 on retinal axon guidance in vitro and retinal axon mapping in vivo. Cell 86:755–766.

Nobes C, Marsh M (2000) Dendritic cells: new roles for Cdc42 and Rac in antigen uptake? Curr Biol 10:R739–R741.

Piper M, Anderson R, Dwivedy A, Weinl C, van Horck F, Leung KM, Cogill E, Holt C (2006) Signaling mechanisms underlying Slit2-induced collapse of *Xenopus* retinal growth cones. Neuron 49:215–228.

Porat-Shliom N, Kloog Y, Donaldson JG (2008) A unique platform for H-Ras signaling involving clathrin-independent endocytosis. Mol Biol Cell 19:765–775.

Praefcke GJ, McMahon HT (2004) The dynamin superfamily: universal membrane tubulation and fission molecules? Nat Rev Mol Cell Biol 5:133–147.

Ray E, Samanta AK (1996) Dansyl cadaverine regulates ligand induced endocytosis of interleukin-8 receptor in human polymorphonuclear neutrophils. FEBS Lett 378:235–239.

Schlunck G, Damke H, Kiosses WB, Rusk N, Symons MH, Waterman-Storer CM, Schmid SL, Schwartz MA (2004) Modulation of Rac localization and function by dynamin. Mol Biol Cell 15:256–267.

Song HJ, Poo MM (1999) Signal transduction underlying growth cone guidance by diffusible factors. Curr Opin Neurobiol 9:355–363.

Sontag JM, Fykse EM, Ushkaryov Y, Liu JP, Robinson PJ, Südhof TC (1994) Differential expression and regulation of multiple dynamins. J Biol Chem 269:4547–4554.

Sun P, Yamamoto H, Suetsugu S, Miki H, Takenawa T, Endo T (2003) Small GTPase Rah/Rab34 is associated with membrane ruffles and macropinosomes and promotes macropinosome formation. J Biol Chem 278:4063–4071.

Swanson JA (1989) Phorbol esters stimulate macropinocytosis and solute flow through macrophages. J Cell Sci 94:135–142.

Swanson JA (2008) Shaping cups into phagosomes and macropinosomes. Nat Rev Mol Cell Biol 9:639–649.

Swanson JA, Watts C (1995) Macropincytosis. Trends Cell Biol 5:424–428.

Tessier-Lavigne M, Goodman CS (1996) The molecular biology of axon guidance. Science 274:1123–1133.

Tojima T, Akiyama H, Itofusa R, Li Y, Katayama H, Miyawaki A, Kamiguchi H (2007) Attractive axon guidance involves asymmetric membrane transport and exocytosis in the growth cone. Nat Neurosci 10:58–66.

Tom VJ, Steinmetz MP, Miller JH, Doller CM, Silver J (2004) Studies on the development and behavior of the dystrophic growth cone, the hallmark of regeneration failure, in an in vitro model of the glial scar and after spinal cord injury. J Neurosci 24:6531–6539.

Trousse F, Marti E, Gruss P, Torres M, Bovolenta P (2001) Control of retinal ganglion cell axon growth: a new role for Sonic hedgehog. Development [Suppl] 128:3927–3936.

van der Bliek AM, Redelmeier TE, Damke H, Tisdale EJ, Meyerowitz EM, Schmid SL (1993) Mutations in human dynamin block an intermediate stage in coated vesicle formation. J Cell Biol 122:553–563.

Wigge P, Köhler K, Vallis Y, Doyle CA, Owen D, Hunt SP, McMahon HT (1997) Amphiphysin heterodimers: potential role in clathrin-mediated endocytosis. Mol Biol Cell 8:2003–2015.

Zheng JQ, Felder M, Connor JA, Poo MM (1994) Turning of nerve growth cones induced by neurotransmitters. Nature 368:140–144.

Zheng JQ, Wan JJ, Poo MM (1996) Essential role of filopodia in chemotropic turning of nerve growth cone induced by a glutamate gradient. J Neurosci 16:1140–1149.